

87
5-11-83 J.S. ①

I-9248

Dr. 1395

UCID-19787

ANALYSIS OF NSWC QUASI-STATIC COMPACTION DATA
FOR POROUS BEDS OF BALL POWDER, MELAMINE, AND
TEFLON, USING STRUCTURAL COMPACTION MODEL

A. M. WESTON
E. L. LEE

Submitted to:
Dr. S. J. Jacobs
Naval Surface Weapons Center
White Oak Laboratory
Silver Spring, Maryland

APRIL 6, 1983

This is an informal report intended primarily for internal or limited external distribution. The opinions and conclusions stated are those of the author and may or may not be those of the Laboratory.

Work performed under the auspices of the U.S. Department of Energy by the Lawrence Livermore Laboratory under Contract W-7405-Eng-48.

Lawrence
Livermore
Laboratory

MASTER

DISTRIBUTION OF THIS DOCUMENT IS UNLIMITED

UCID--19787

DE83 012043

ANALYSIS OF NSWC QUASI-STATIC COMPACTION DATA
FOR POROUS BEDS OF BALL POWDER, MELAMINE, AND
TEFLON, USING STRUCTURAL COMPACTION MODEL*

A. M. Weston
Wm. Brobeck and Associates

E. L. Lee
Lawrence Livermore National Laboratory
University of California
Livermore, California 94550

ABSTRACT

A "structural" compaction model is used to correlate NSWC quasi-static compaction data on porous beds of six(6) different materials, i.e., four(4) ball powders, melamine, and Teflon. Initial densities of the porous beds ranged from 44 percent solid "theoretical maximum density" (TMD) to 70 percent TMD. Maximum compacted densities were about 90 percent TMD except for Teflon which was compacted to approximately 98 percent TMD. Pressures calculated by the model, plotted as a function of percent TMD, agree well with the NSWC data.

DISCLAIMER

This report was prepared as an account of work sponsored by an agency of the United States Government. Neither the United States Government nor any agency thereof, nor any of their employees, makes any warranty, express or implied, or assumes any legal liability or responsibility for the accuracy, completeness, or usefulness of any information, apparatus, product, or process disclosed, or represents that its use would not infringe privately owned rights. Reference herein to any specific commercial product, process, or service by trade name, trademark, manufacturer, or otherwise does not necessarily constitute or imply its endorsement, recommendation, or favoring by the United States Government or any agency thereof. The views and opinions of authors expressed herein do not necessarily state or reflect those of the United States Government or any agency thereof.

DISTRIBUTION OF THIS DOCUMENT IS UNLIMITED

leg

INTRODUCTION

The porous material, compaction model is illustrated on Fig. 1. Associated equations are derived in reference 1. The model is based upon the collapse of a spherical pore similar to that described by Carroll and Holt.² Radial inertia and strain rate dependence are ignored. It does include trapped gas inside the pore, and a solid material flow stress difference that can be a "strain hardening" function of porosity. This creates both a yield point and a variation in stress with radius around the pore. Elastic behavior of the porous material is governed by a bulk modulus definition that can fit data from different kinds of materials, from structural foams to compacted aggregates of flexible particles.

FORMULATION OF THE MODEL

The behavior of the model is best explained in relation to relative density, which is a function of porosity, α , mean solid material density, ρ , and initial mean solid material density, ρ_0 .

Subscript "0" refers to initial conditions

$$TMD = 100 \frac{\rho}{\rho_0} \left(\frac{1}{\alpha} \right) \quad (1)$$

Porosity is defined by cell dimension a , and pore diameter, d .

$$\alpha = \left[1 - \frac{\pi}{6} \left(\frac{d}{a} \right)^3 \right]^{-1} \quad (2)$$

The cell dimension is related directly to relative density and initial relative density.

$$a = a_0 \left[\frac{TMD_0}{TMD} \right]^i ; \text{ where,}$$

$i = 1/3 \text{ for cubic compression}$

$i = 1 \text{ for 1D constant strain compression}$

(3)

The density of the matrix material increases slightly with intragranular* compaction pressure. At the low intragranular pressures corresponding to the quasi-static compaction data range here, ρ does not increase from its initial value significantly. However, for pore closing pressures when relative density is in excess of 90 percent TMD, the increase in ρ can no longer be ignored.

There are three regimes of compaction behavior, i.e.¹, initial elastic,² pore closing flow,³ and locked up elastic. In the initial elastic regime, intragranular pressure, τ_i , increases above ambient pressure, P_a , as the porous elastic volume, v , decreases. The increase is determined by a bulk modulus that in turn is a function of porosity and pore gas pressure, P_g .

$$\tau_i = - \int_{V_0}^V K(a, P_g) \frac{dv}{v} + P_g \quad (4)$$

Pore gas pressure is a function of initial and current pore diameters and a gas compression process constant k .

* The term "intragranular stress (pressure)" is taken from references 6 and 7 in which the NSWC compaction data is described. It's meaning is the same as, "mean isostatic pressure."

$$P_g = P_a \left(\frac{d_0}{d} \right)^{3k} \quad (5)$$

To match the quasi-static data illustrated here, k , the gas compression process constant, was set at the isothermal value of 1.0. This varies from reference 1 were k was set at a dry air isentropic value of 1.4. The elastic bulk modulus $K(\alpha, P_g)$, is,

$$K(\alpha, P_g) = \frac{K_s}{\alpha} \exp\left(-2C\frac{\alpha-1}{\alpha}\right) + kP_g\left(\frac{\alpha-1}{\alpha}\right) \quad (6)$$

The solid material bulk modulus, K_s , increases with pressure. As for solid density at the low pressures corresponding to the quasi-static compaction data, K_s does not increase significantly over its initial value. For pore closing pressures when relative density is in excess of 90 percent, the increase in K_s can no longer be ignored. Linear Hugoniot constants for the solid material are used in derived equations that quantify the increase of K_s and ρ , with pressure. See reference 1 for details.

The exponential multiplier on K_s in equation 6 permits the fitting of the initial elastic behavior for a wide variety of porous materials. Kooker and Anderson³ suggested the form of this multiplier based on experimental acoustic data of Elban⁴ and the ceramic compaction data of Knudsen.⁵ When the constant, $C = 0$, a structural foam is modeled. When the constant, $C > 0$, non-linear contact behaviors of discrete particles packed together are modeled. A value of $C = 2.2$ will yield results that approximate the Carroll and Holt² model. When $C \gg 0$, elastic pore closure can be approximated.

When the pressure from equation 4 exceeds a yield value, the pore closing flow regime begins. In this regime, intragranular pressure, τ_i , is controlled by a mechanical flow stress equation.

$$\tau_i = Pa \left(\frac{d_0}{d} \right)^{3k} + \pi H \left(\frac{d}{a} \right)^3 \left[\frac{1}{3} \left(\frac{a}{d} \right)^3 \left(\ln \frac{a}{d} - \frac{1}{3} \right) + \frac{1}{9} \right] + \left(2 - \frac{\pi}{3} \right) H \ln \frac{a}{d} \quad (7)$$

The parameter, H , is the difference between radial and tangential pressure in a one dimensional spherical pressure field centered on a pore. Numerically, the value of H is approximated by the flow stress measured in a uniaxial 1D stress compression test on a bar of 100 percent TMD material with a large length to diameter ratio. The results of Hopkinson bar compression experiments yield an approximate mapping of H as a function of strain and strain rate.

Here values of H were selected to fit the compaction data. The porous compaction data spans six materials, i.e., from ball powders to melamine, and Teflon. The ball powder data were fitted quite well using a constant value for H . The Teflon and melamine data were fitted using a value of H that increases with compaction. This strain hardening behavior is expressed as,

$$H = H_0 \left\{ 1 + B \left[\left(\frac{a}{d} \right)^N - 1 \right] \right\} \quad (8)$$

Total compaction is the sum of an elastic component and a pore closing flow component. The pore closing flow pressure from equation 7 becomes indefinitely large as the pore diameter becomes indefinitely small. Consequently, as solid density is approached, equation 7 no longer controls pressure; instead the pores "lock up" and the compaction behavior is controlled by the bulk compressibility of the solid material, K_s .

COMPARISONS OF CALCULATED AND EXPERIMENTAL RESULTS

The published NSWC data^{6,7} is presented in two formats, as a semi-log plot of intragranular compaction pressure versus percent TMD, and as a log-log plot of compaction pressure versus the quantity, percent TMD minus initial percent TMD. While the log-log plot results in straight line data plots, it masks the essentially elastic-plastic nature of the data. Also, to compare on one graph, different sets of data starting from different values of initial percent TMD, the log-log plots were transformed to the semi-log format with linear percent TMD as the abscissa. Figure 2 illustrates the NSWC semi-log data plot for WC 231. Figure 3 illustrates the NSWC log-log data plot for WC 140, and also a transformed semi-log plot.

The computer program that represents the calculation model used here, is programmed to plot pressure versus percent TMD in semi-log format similar to the first mode of NSWC data presentation. Six points representing NSWC data at different values of percent TMD are plotted and compared to the curve calculated from the model. The NSWC data are numerous. These six "comparison points" are (1) approximately averaged data clusters, or (2) values from the NSWC least squares data fit. Figures 4 and 5 illustrates the computer outputs that correspond to Figs. 2 and 3.

Figures 2 through 7 illustrate model results versus NSWC data for four(4) ball powders, WC 231, WC 140, Olin Type A Fluid, and Olin TS 3660. For these materials the constants B and N in equation (8) are zero; pore closing flow is characterized adequately by a single value for solid material flow stress, H.

Data for Winchester ball powder⁶, WC 231, is first illustrated. These data began at an initial density of 44 percent TMD, a value that is below, but approximately equal to the minimum model density of 47.64 percent TMD. The model is a cubic array of spherical pores in a matrix of solid material. These pores interfere at less than 47.64 percent TMD when the pore diameter equals the cell size. At lesser density the model becomes a collection of pieces that do not touch. Except for a small component for bulk gas compression, the model will predict ambient pressure for all densities less than 47.64 percent TMD.

For the entire ball powder data range, the compaction pressures are sufficiently low for the solid matrix density, ρ , to approximately equal its initial value, ρ_0 . To illustrate this the calculated model line on Fig. 4 includes bulk compressibility while the calculated line on Fig. 2 does not. Similarly the calculated model line on Fig. 5 includes bulk compressibility while the calculated line on Fig. 3 does not.

Figure 8 is a computer code output for Teflon⁷ (15g, 25g samples) when a constant value for H is used. The data correlation is poor. Figure 9 shows the results when the parameters B and N in equation 7 are allowed to be non-zero, i.e., H increases with compaction. The data correlation is much improved. Teflon is mildly "strain hardening."

Figure 10 shows results for melamine⁷ (15g sample) when a constant value for H is used. The data correlation is again poor. Figure 11 is a much improved computer code output when parameters B and N have very high values. Melamine "strain hardening" is severe.

In estimating calculation model elastic parameters, the constant C in equation 6 was selected arbitrarily to fit the data. The solid matrix bulk modulus, K_s , was estimated from shock Hugoniot velocity data. The nitrocellulose ball powder Hugoniot data was assumed to be like pyroxylin from reference 8. The Teflon Hugoniot data was from reference 9. The Melamine Hugoniot data was assumed to be like TNT from reference 10.

For the six materials considered, the elastic and flow parameters used to characterize the compaction behavior are tabulated in Table 1.

DISCUSSION

In correlating the compaction data, the effect of solid matrix compressibility is important only for the Teflon data which was compressed to a final density of 98 percent TMD. All the remaining data, including the Teflon data at less than approximately 90 percent TMD, can be correlated using constant initial values for solid matrix density, $\rho = \rho_0$, and bulk modulus, $K_s = K_{s0}$. The effect of ignoring compressibility, is illustrated in Fig. 12. The dotted line represents incompressible WC 231. As ρ approaches ρ_0 the pressure required to approach 100 percent TMD becomes (incorrectly) large without limit.

Consider a loosely packed porous bed that is loaded, compacts irreversibly to a higher density, and then is unloaded. When reloaded the pressure will first increase with small change in density, i.e., elastically, until the yield limit (represented here by the solid line pore closing flow pressure from equation 7) is reached. With further loading, the solid material will again begin to flow, the pores will

further close, and the density will rapidly increase along the yield limit line. This process is also illustrated in Fig. 12 showing calculated compaction to the yield limit line from various levels of initial compaction.

Figure 13 shows a mapping of yield (flow) lines for differing values of matrix flow stress, for materials with solid matrix bulk properties similar to ball powder. The bounding line at the bottom labeled "isothermal pore gas pressure" corresponds to the case where the matrix flow stress is zero. Note how it, and all other yield (flow) lines join a single limit line when at high pressure, the solid matrix density exceeds 100 percent TMD.

Since the compaction model is based upon the notion of pore closing "flow", we attribute compaction data that aligns with softer ball powder materials shown in the Fig. 13 mapping, to a "flow" mechanism. On the other hand, compaction data for melamine, Fig. 10 crosses these curves at a significant angle, indicating that in addition to deforming flow, a strain hardening mechanism is operating. For example, the melamine may be "fracturing", i.e., making an increased number of smaller particles as it is compacted.

REFERENCES

1. A. M. Weston and E. L. Lee, "A Constitutive Model for Porous Materials," Propulsion System Hazards Meeting, China Lake, Ca., April 27, 1982, UCRL-87450.
2. M. M. Carroll, and A. C. Holt, "Static and Dynamic Pore-Collapse Relations for Ductile Porous Materials," J. Appl. Physics, 43(4), pp. 1626-1636 (1972).
3. D. E. Kooker, and R. D. Anderson, "A Mechanism for the Burning Rate of High Density, Porous, Energetic Materials," 7th Symposium on Detonation.
4. W. L. Elban, NSWC, unpublished data, 1980.
5. F. P. Knudsen, "Dependence of Mechanical Strength of Brittle, Polycrystalline Specimens on Porosity and Grain Size," J. Amer. Ceramic Soc., Vol. 42, No. 8, pp. 376-387, 1959.
6. NSWC HEPS Technical Progress Report, January 27, 1982, W. L. Elban, "Quasi-Static Compaction of Porous Beds," Figs. 5, 6, 7, 14, and 18, pp. 2-31.
7. H. W. Sandusky, W. L. Elban, K. Kim, R. R. Bernecker, S. B. Gross, A. R. Clairmont, "Compaction of Porous Beds of Inert Materials," 7th Detonation Symposium, June 16-19, 1981, pp. 444 and 456, Figs. 8 and 9.
8. Veretennikov, Dremin, Shvedov, "Shock Compressibility of NB Powder in Porous and Un-Porous States," Combustion Explosion and Shock Waves, Vol. 5, No. 4, pp. 342-345, 1969.
9. M. Van Thiel, "Compendium of Shock Wave Data," UCRL 50108, 1967, Vol. 3, Data for Teflon, 23-9(2-4) ---3.
10. M. Van Thiel, "Compendium of Shock Wave Data," UCRL 50108, 1967, Vol. 3, Data for TNT, 23-18-2-1(7-3-5-6) ---7.

TABLE 1 Compaction Model Input Parameters to match NSWC quasi-static data arrays

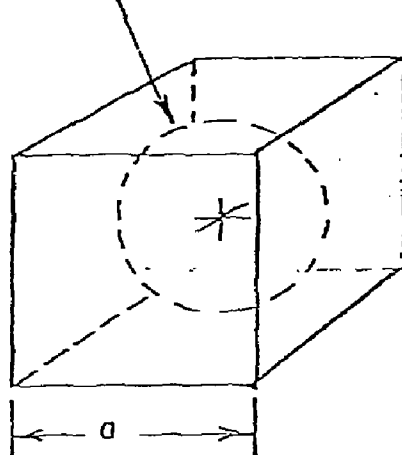
Material	TMD	Elastic Regime				Flow Regime			Mean Particle Dia. mm
		ρ_0 g/cc	c mm/c.s	s	C	H_0 GPa	β	κ	
WC23I	47.65	1.63	1.7	1.85	3.5	0.060	0.	0.	.7874
WC140	57.8	1.63	1.7	1.85	3.5	0.165	0.	0.	.4115
Olin Type A	60.0*	1.63	1.7	1.85	4.5	0.130	0.	0.	.045
TS3660	56.2	1.63	1.7	1.85	4.0	0.108	0.	0.	.7137
Teflon 7C	66.0**	2.305	1.88	2.07	5.0	0.0089	1.0	0.75	>.055
Melamine	69.5**	1.543	2.66	1.826	5.0	0.0038	3.2	4.0	.055

* NSWC stated an initial density of 56.2 percent TMD, reference 6.

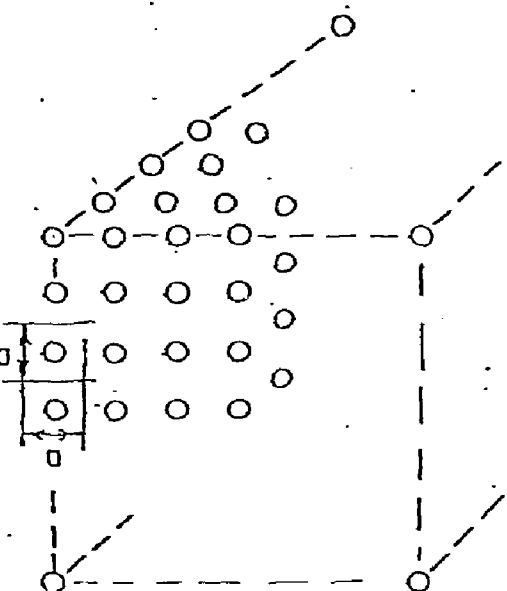
** Estimated from NSWC data plots, reference 7.

BULK COMPACTION MODEL GEOMETRY

PORE DIA., d , GAS FILLED

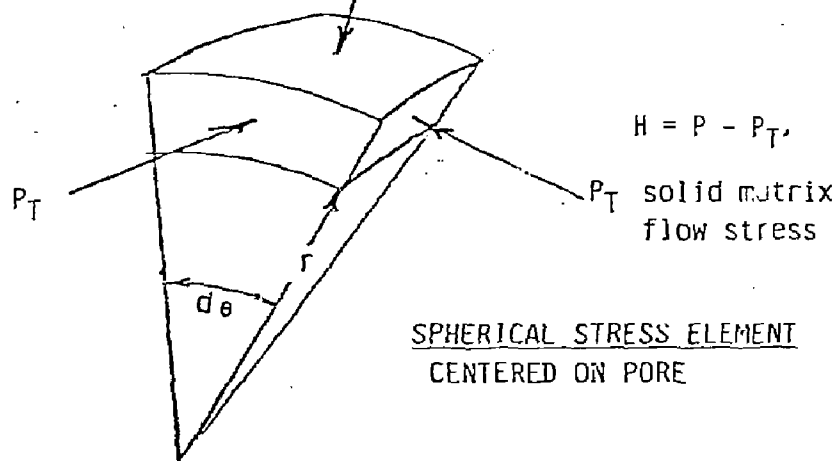


COMPACTION CELL



SQUARE ARRAY OF CELLS

$P + \frac{dP}{dr} dr$, Radial Pressure



SPHERICAL STRESS ELEMENT
CENTERED ON PORE

FIG. 1

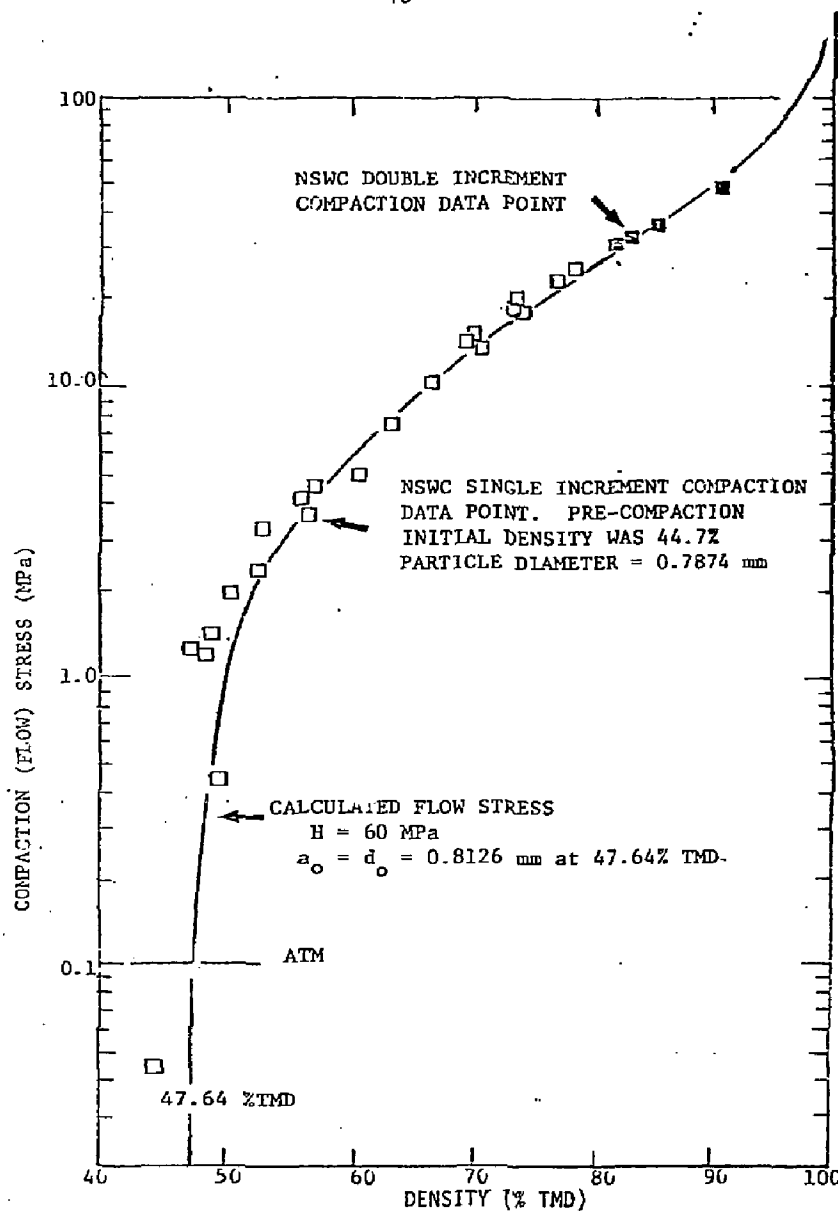
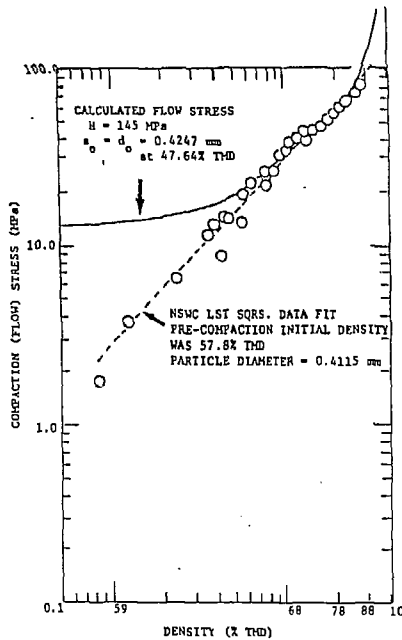


Fig. 2 Analytical mechanical flow stress and NSWC intergranular stress data versus density for 12 g Winchester 231 ball powder.



$$[\% \text{ TMD} = \langle (\% \text{ TMD})_0 \rangle]$$

Fig. 3a Analytical mechanical flow stress and NSWC intragranular stress data versus density for 15 g Olli. WC140 ball powder.

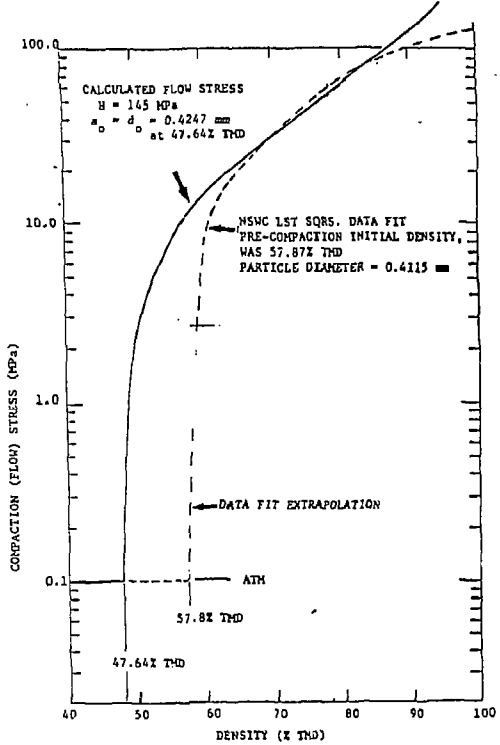


Fig. 3b Analytical mechanical flow stress and NSWC LST SQRS. intragranular stress data fit versus density for 15 g Olli. WC140 ball powder.

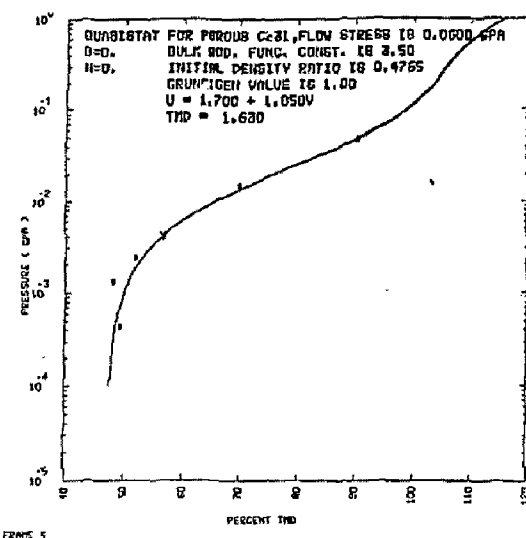


Fig. 4

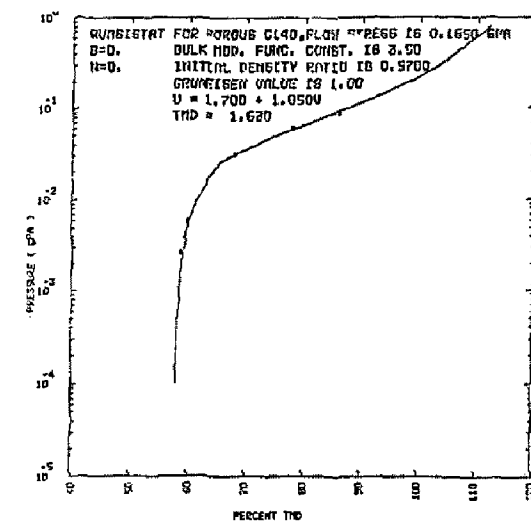


Fig. 5

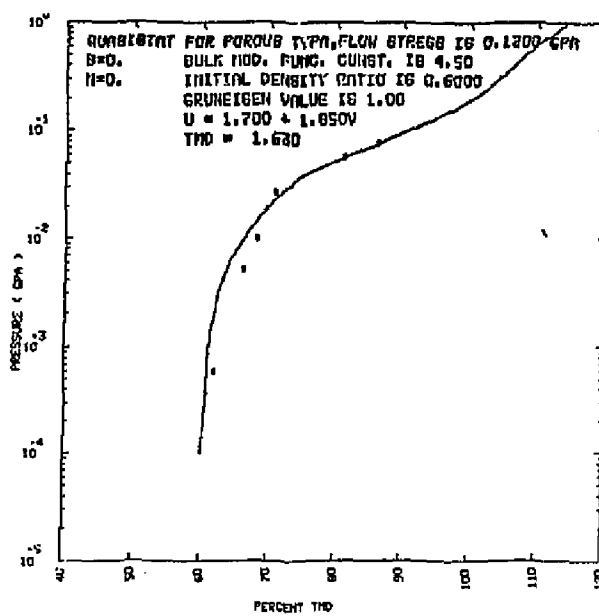


Fig. 6

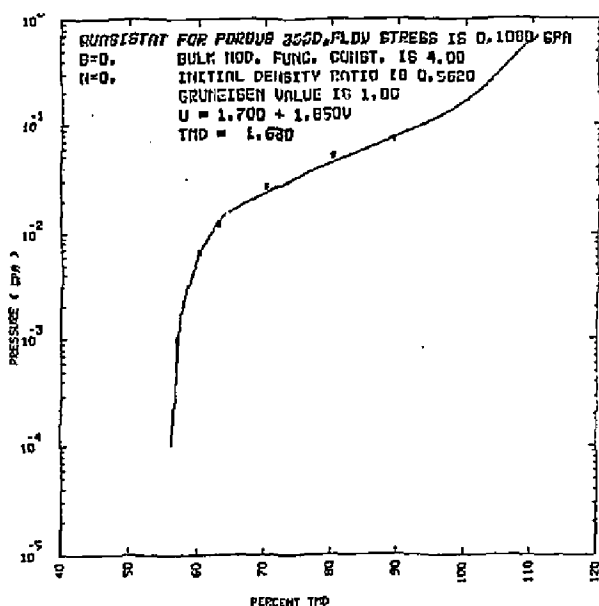
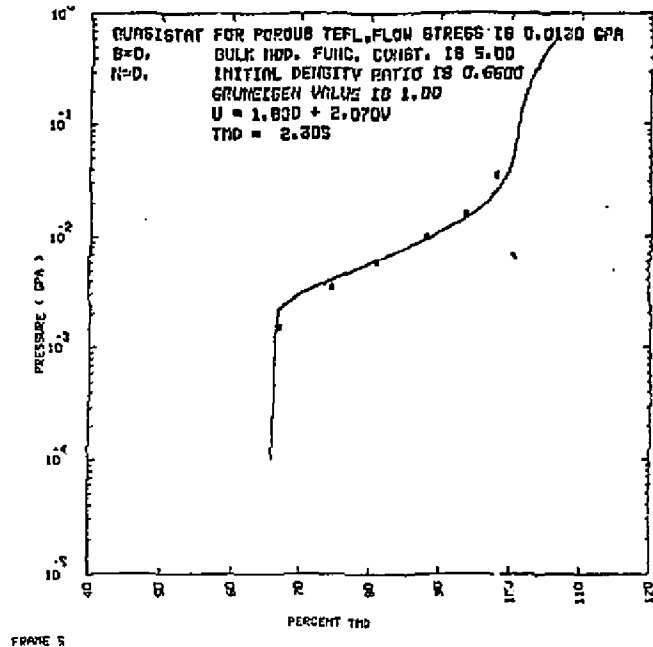
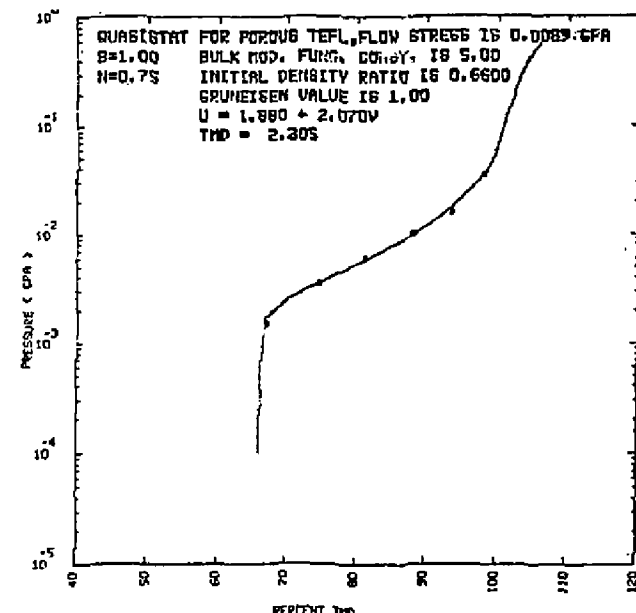


Fig. 7



FRAME 8

Fig. 8



FRAME 8

Fig. 9

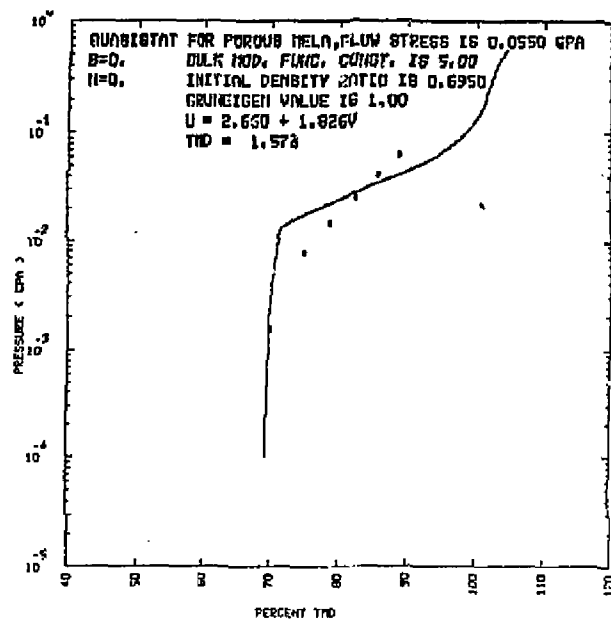


Fig. 10

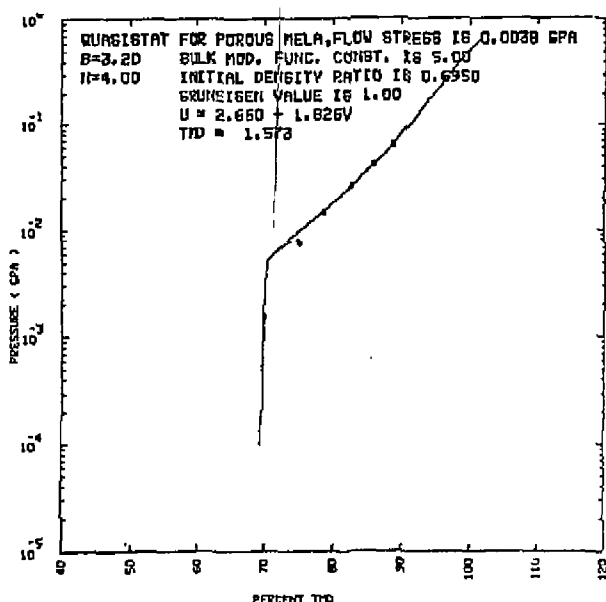


Fig. 11

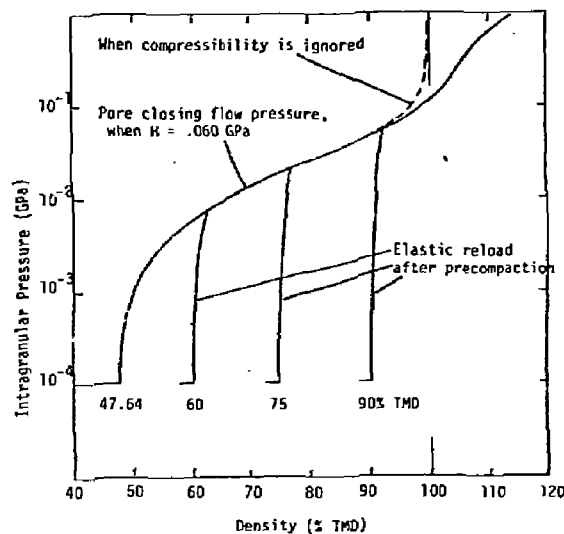


Fig. 12 Pore closing flow pressure versus density for WC231, illustrating the effects of compressibility and precompaction.

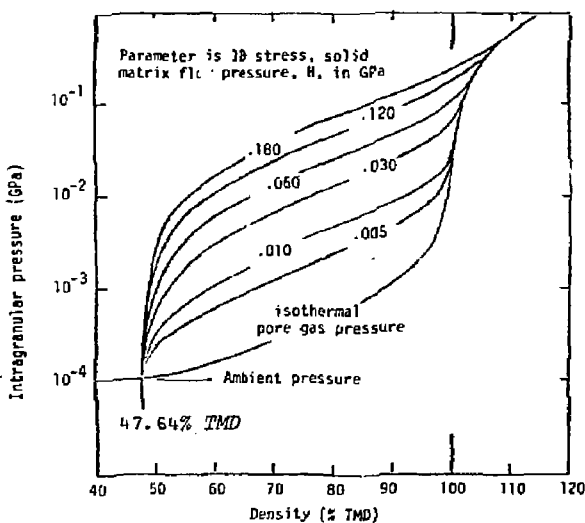


Fig. 13 Pore closing flow pressure versus density and solid matrix flow pressure, for ball powder type materials.